

Article

Non-Invasive Intraoral Stand-Alone Tongue Control System Based on RSIC-V Edge Computing

Lijuan Shi ^{1,2,3}, Xiong Peng ¹, Jian Zhao ^{2,3,4,*}, Zhejun Kuang ^{2,3,4} , Tianbo An ^{2,3} and Liu Wang ^{2,3}

¹ College of Electronic Information Engineering, Changchun University, Changchun 130012, China; shilj@ccu.edu.cn (L.S.); pengxiong11@163.com (X.P.)

² Jilin Provincial Key Laboratory of Human Health Status Identification Function & Enhancement, Changchun 130022, China; kuangzhejun@ccu.edu.cn (Z.K.); antb@ccu.edu.cn (T.A.); wangliuclg@163.com (L.W.)

³ Key Laboratory of Intelligent Rehabilitation and Barrier-Free for the Disabled, Changchun University, Ministry of Education, Changchun 130012, China

⁴ College of Computer Science and Technology, Changchun University, Changchun 130012, China

* Correspondence: zhaojian@ccu.edu.cn

Abstract: The intelligent tongue control system is of great significance for assisting the independent life of patients with a limb disability. In order to more accurately control the assisted living equipment of incompetent patients and solve the power-loss problem of the intelligent tongue control system, this research designs a non-invasive pressure sensor array for tongue touch signal detection in the oral cavity and proposes a tongue control system based on RSIC-V edge computing. The system converts the tongue touch pressure data into specific control instructions on the edge of the RSIC-V chip and transmits them to the receiver, thus reducing the transmission of data. This study takes control of the wheelchair motor as the test object. In the experiment, the speed response time test, the center click task, and the power consumption experiment are carried out, whose results show that the adaptive fuzzy PID control algorithm has good robustness in the system; when the DC motor with a given speed of 750 r/min reaches the steady state, its rise time is 0.108 s and the adjustment time is 0.59 s. The dynamic power consumption of the non-intrusive intraoral stand-alone tongue control system proposed in this paper is found to be 3.745 MW, which is 11.5% lower than the total power consumption of the sTD system.

Keywords: tongue control system; RSIC-V; flexible carbon nanotube PDMS; edge of computing



Citation: Shi, L.; Peng, X.; Zhao, J.; Kuang, Z.; An, T.; Wang, L.

Non-Invasive Intraoral Stand-Alone Tongue Control System Based on RSIC-V Edge Computing. *Appl. Sci.* **2023**, *13*, 9490. <https://doi.org/10.3390/app13179490>

Academic Editors: Dimitris Mourtzis and Ki-Yong Oh

Received: 2 May 2023

Revised: 31 July 2023

Accepted: 16 August 2023

Published: 22 August 2023



Copyright: © 2023 by the authors. Licensee MDPI, Basel, Switzerland. This article is an open access article distributed under the terms and conditions of the Creative Commons Attribution (CC BY) license (<https://creativecommons.org/licenses/by/4.0/>).

1. Introduction

According to the statistics, there are 85 million disabled people in China currently, among whom there are 25 million patients with functional disabilities of upper and lower limbs, and number of patients with physical disabilities and disabilities caused by congenital, disease, natural disasters, and traffic accidents is increasing year by year. The number of seniors over the age of 60 is 241 million, and with the severity of aging, the size of the disabled elderly population with quadriplegia caused by spinal cord injury, cerebral palsy, stroke, etc., continues to expand [1]. In order to solve the problems of assisted life for incompetent patients with upper and lower limb disability, researchers have carried out related research such as intelligent brain control, eye control, tongue control auxiliary system, etc., in which the tongue system can more accurately provide complex movement control and manipulation ability because it has a high degree of flexibility and is not affected by the human posture [2]. Therefore, it is of great significance to explore the tongue-controlled interactive assistance technology to help incompetent patients with limb disability have a relatively independent living ability and improve quality of life accordingly.

Relevant Work

The control problems of the tongue control system mainly focus on power loss and control accuracy issues. Currently, popular tongue control research protocols include the low-power independent system of tongue drive (iSTD) based on the magnetic array, extraoral tongue drive system (ETDS), and joystick-controlled tongue control intelligent assistive device (STD) [3–5]. For iSTD systems, any bumps on a wheelchair of the patient may lead to the misoperation of magnetic beads on the tongue and cause the control unit to emit misoperation signals, and ETDS and STD sometimes have similar problems. In addition, the above three methods only involve the simple control of wheelchairs in the direction of front, back, left, and right without optimizing the subsequent smoothing control of a wheelchair's specific motion speed.

To solve this problem, we propose a non-invasive intraoral stand-alone tongue control system based on RSIC-V edge computing by using the Rocket processor as the edge node decision-maker to obtain communication with low power consumption and low bandwidth while maintaining a reasonable cost. By setting the pressure threshold and changing the amount of pressure, the wheelchair is controlled by closed-loop fuzzy PID, so as to avoid the malfunction of the control unit and optimize the users' experience [6]. The structure diagram of the non-invasive intraoral independent tongue control system based on RSIC-V edge computing is shown in Figure 1 below.

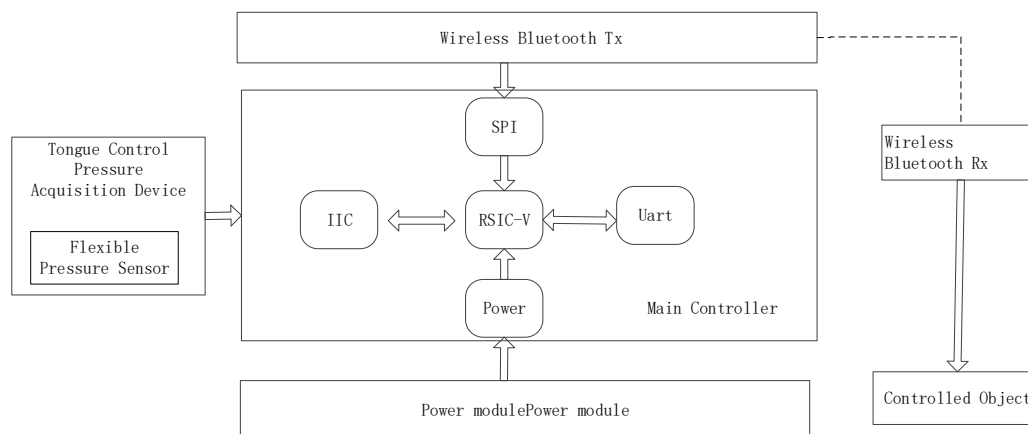


Figure 1. The structure diagram of the non-invasive intraoral independent tongue control system based on RSIC-V edge computing.

2. System Hardware Architecture

2.1. Master Controller

Due to the particularity of the oral environment, the master control chip placed in the oral cavity for monitoring the tongue muscle pressure needs to have the characteristics of stability, small size, light weight, low power consumption [7], and supporting wireless communication to adapt to the particularity of the oral environment and provide an effective means to monitor tongue control devices. Consequently, the controller adopts the RSIC-V chip based on the Rocket kernel [8], and the characteristics of modularity make RISC-V have the characteristics of miniaturization and low energy consumption, which is crucial for embedded applications, as shown in Figure 2. The dynamic power of the Rocket kernel is 0.034 mW/MHz, which is manufactured by TSMC (Taiwan Semiconductor Manufacturing Company Limited, Taiwan, China) 40GPLUS technology and its area is 0.14 mm². In comparison, the Arm Cortex-A5 (Arm Technology (China) Co., Ltd., Shanghai, China) (32-bit single-phase order) manufactured with the same process has a dynamic power of 0.08 mW/MHz and an area of 0.27 mm². Running at the same frequency (>1 GHz), the 64-bit Rocket scalar kernel consumes less power than the A5 kernel. To reduce power consumption, a power management unit is added to the SoC on the RSIC-V chip. If the

SoC or a certain domain of the SoC is not used at certain times or in some applications [9], the power management unit will lower the voltage.

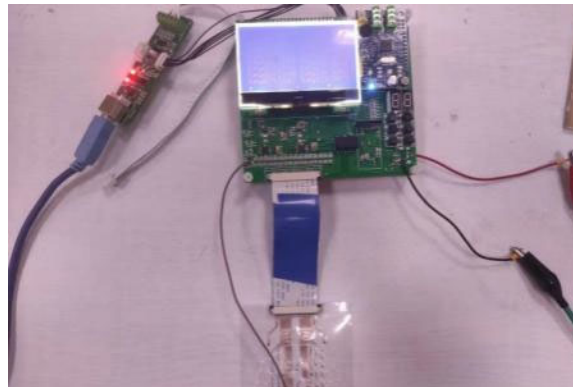


Figure 2. RSIC-V system board.

2.2. Pressure Sensor Array Designing for Tongue Touch Signal Detection

Compared with traditional pressure sensors, flexible thin-film pressure sensors are more suitable for closed and humid environments in the mouth. Thus, we use a carbon nanotube-PDMS resistive pressure sensor array to integrate a signal conditioning circuit next to the pressure sensor bridge. Because this pressure sensor uses the inter-integrated circuit (I2C) communication protocol, all six sensors are connected to the same data and clock bus [10], as shown in Figure 3. The I2C protocol specifies that the data and clock bus connect a pull-up resistor between the bus and the power supply, and Ohm's Law is used to determine the minimum pull-up resistor required for the I2C connection. At this stage, there are no timing requirements; therefore, the minimum value of the pull-up resistor used is 4.7 k. A 3.7 V DTP301120 polymer Li-ion is used to power electronics. The carbon nanotube-PDMS resistance pressure sensor is shown in Figures 3–5, showing the layout of the pressure sensor on the artificial palate film.

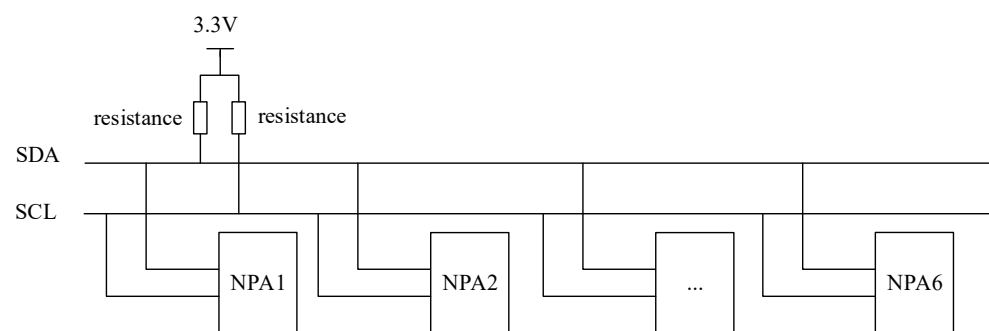


Figure 3. Carbon nanotube-PDMS pressure sensor connected by iic bus.

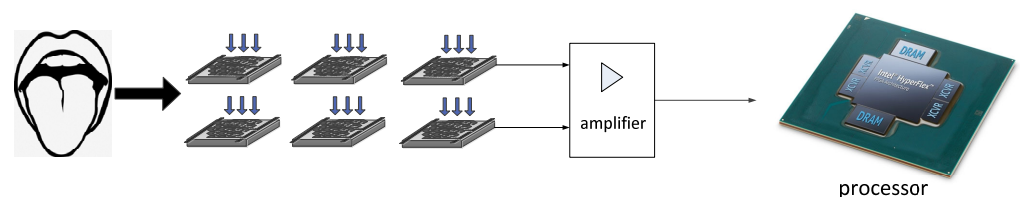


Figure 4. Carbon nanotube-PDMS sensor and controller interface.

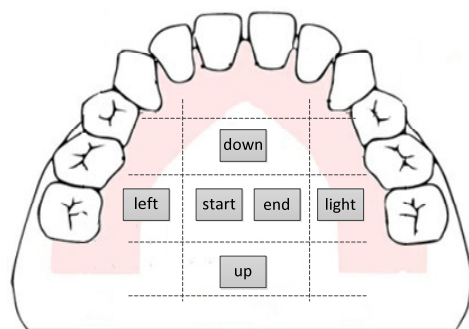


Figure 5. Layout of pressure sensor in artificial palatal film.

2.3. Generation and Transmission Mode of Control Commands for Tongue Pressure Signals

Compared with *etds*, the challenge of this method lies in embedding flexible pressure sensors in a wet oral environment, and the collected pressure signals generate specific action commands through the signal conditioning circuits, and finally, the action commands are transmitted to the wheelchair-side wireless receiver through a wireless communication module. In order to solve the problems of Tx antenna impedance and RF loss, Ali Jafari et al., put forward several ideas [11]. Here, we used a custom-designed intraoral antenna to address this issue. Also, in previous *iTDS* and *eTDS* versions, raw magnetic sensor data had to be sent wirelessly to the Rx, and then processed and converted to tongue commands on a PC or smartphone. In this new design, an efficient tongue command detection algorithm processes raw data inside the tongue cavity and generates tongue commands directly in real time without relying on Rx processing power or software. By reducing the amount of data sent wirelessly to Rx, the intralingual pressure sensor data node is independent, and the power consumption of the system is reduced. Furthermore, by standardizing motion commands to match the standard format of Human Interface Devices (HIDs), they can be universally accepted as peripherals by most of today's computing devices [12].

3. Data Acquisition and Processing of Tongue Control Signal Based on RSIC-V Edge Computing

3.1. Pressure Data Processing Nodes and Transmission

The system edge node is shown in Figure 6 below, whose design consists of four parts: data acquisition part, data processing part, master controller, and wireless transmission. Pressure sensors are distributed on the edge to collect raw pressure data, which is subsequently transmitted to the RSIC-v processor in parallel through the signal conditioning circuit. Due to the parallel transmission mode, the number of pressure sensor nodes will not affect the system data transmission rate. The signal conditioning circuit is mainly composed of a differential mode amplifier and filter. The third part is the finite state machine (FSM), which is a kind of computing model abstracted to study the computation process of finite memory and some language classes. A finite state automaton has a finite number of states, each of which can transmit to zero or more states, and the input string determines which transmission state is performed. This module converts pressure data into action instructions, and it is also the decision-maker of the whole system, which processes all data from sensors and combines them with triggers from the cloud, and then the FSM determines the state of the environment around the node [13]. For example, if the pressure signal is less than the set action threshold, then the decision-maker will judge it as invalid, and the system does not issue any action commands. The AES encryptor is the third part of this edge Internet of Things, which guarantees the security of data transmission. All data from the FSM unit are encrypted before the nodes are transmitted to the cloud. In this paper, the 128-bit version of the RSA module is employed. The last part of the edge node is the wireless transceiver module, which transmits the encrypted output from the node to the cloud [14]. The transceiver module can also send some defined information or instructions to the node from the cloud. In this paper, we use node 2.4 GHz high-gain antenna as

the wireless transceiver module. The wireless sending nodes only need to transmit the modulated action command without transmitting a large amount of raw pressure data, which makes the system require low throughput.

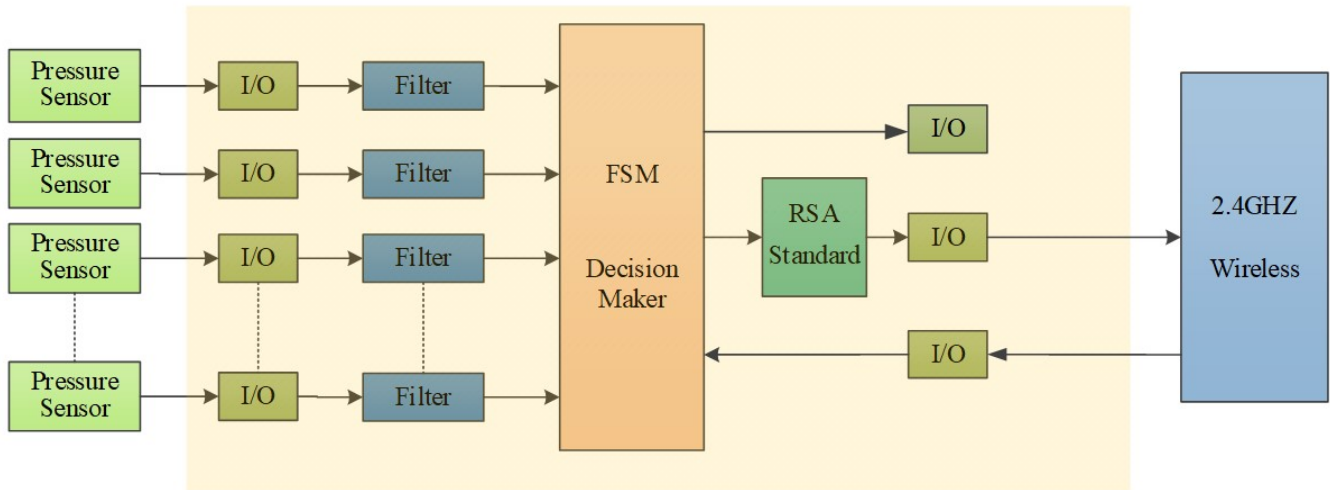


Figure 6. Edge Internet of Things (IoT) node block diagram.

3.2. Tongue Touch Signal Control Command Transmission

The software architecture of the tongue control auxiliary device includes two modules: the software design of the intraoral stand-alone unit and the software design of the extraoral stand-alone unit. For the intraoral stand-alone unit, the communication mode between the CNT-PDMS pressure sensor array and the data-processing unit is iic. Firstly, establish the communication between master and slave machines according to the device address and configure the wireless transmitter Rx. When the pressure sensor captures the pressure signal, the wireless transmitter can choose to send the original pressure data or send the action signal that has been processed by the data-processing unit. Considering that if the original pressure data is sent, more resources and power consumption will be consumed, thus we choose to send the processed action signal directly through Rx. For the extraoral independent unit, communication with the intraoral independent unit needs to be established first. When the wireless receiver Tx receives the action information, the master control chip transmits this action information to the wheelchair through Rx to control the movement of the wheelchair. The intracavitary independent unit software is shown in Figure 7 below. When the pressure sensor detects that the current pressure is larger than the set threshold, the pressure signal is employed to control the PWM of the wheelchair motor through adaptive fuzzy PID to ensure the smooth movement of the wheelchair and increase the comfortability of users.

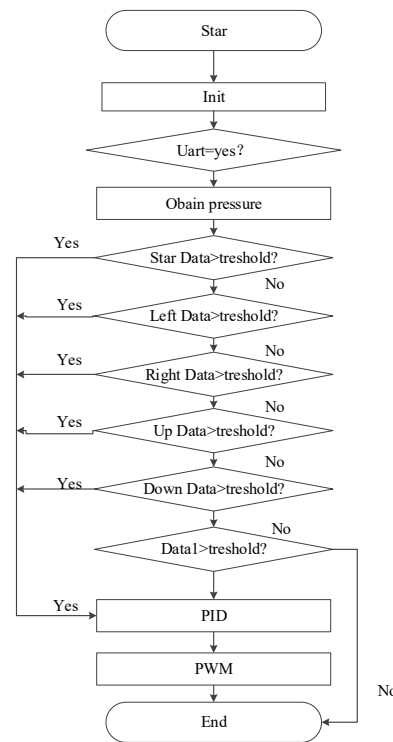


Figure 7. Software flow diagram.

4. Tongue Control System Control Algorithm

4.1. PID Control of Tongue Control System

What is introduced above is mainly the information-collection method adopted by the tongue control device. For a comprehensive control system, follow-up control methods should also be considered. In engineering practice, the most widely used regulator control law is PID control. Izci D introduced the design of an optimized proportional integral differential (PID) controller for speed control of direct current (DC) motors. By multiplying the time integral by the absolute error objective function, the optimal value of PID gain was obtained. This method performs well in transient and frequency response, as well as robustness and anti-interference, and different practical algorithms are used to adjust the controller [15,16]. When the structure and parameters of PID regulating controlled object cannot be fully mastered or there is no accurate mathematical model, the structure and parameters of the system controller must be determined through experience and field debugging [17].

In practice, there are also PI and PD controls in PID control. PID controller is a systematic error, which is controlled by proportional, integral and differential calculations of the control quantity. When the pressure of the tongue muscle touching the pressure sensor changes, the movement of the wheelchair is also approximately uniform or uniformly accelerated and decelerated accordingly, allowing the user to feel more comfortable during the movement. The flow chart of the traditional PID algorithm is shown in Figure 8 below.

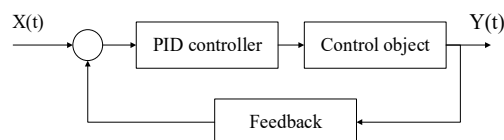


Figure 8. PID algorithm flow diagram.

The specifications of the wheelchair DC motor are as follows: rated voltage $U_N = 24\text{ V}$, rated current $I_N = 13.7\text{ A}$, maximum speed $n_N = 750\text{ r/min}$, allowable overload factor

= 1.6, the amplification factor of the thyristor triggered rectifier: $K_s = 100$, loop resistance $R = 10 \Omega$, electromagnetic time constant: $T_1 = 0.04 \text{ s}$. Current feedback coefficient $\beta = 0.3$. PI type is selected for the current regulator, and its transfer function is

$$W_{ACR} = K_i \frac{1 + \tau_i S}{\tau_i S} \tag{1}$$

ACR preemptive time constant: $\tau_i = 0.04\text{s}$. The scale factor of ACR is

$$K_i = K_i \frac{\tau_i R}{K_S R} = 22.3 \times \frac{0.04 \times 10}{100 \times 0.3} = 0.293 \tag{2}$$

$$W_{ACR} = K_i \frac{1 + \tau_i s}{\tau_i s} = 0.293 \times \frac{1 + 0.04s}{0.04s} \tag{3}$$

PI type is selected for the current loop ASR regulator, and its transfer function is

$$W_{ASR} = K_n \frac{1 + \tau_n S}{\tau_n S} \tag{4}$$

Taking $m = 5$, the lead time constant is

$$\tau_n = m T_{\Sigma n} = 5 \times 0.016 = 0.08\text{s} \tag{5}$$

Speed loop open loop gain:

$$K_N = \frac{m + 1}{2m^2 T_{\Sigma n}^2} = \frac{6}{2 \times 25 \times 0.00025} = 76 \tag{6}$$

$$W_{ACR} = K_i \frac{1 + \tau_i s}{\tau_i s} = 25 \times \frac{1 + 0.08s}{0.08s} \tag{7}$$

4.2. Fuzzy PID Control of Tongue Control System

The intelligent wheelchair is a multi-variable, nonlinear, time-varying system, which requires high accuracy and robustness, while it is difficult for traditional PID controllers to achieve this goal. Fuzzy PID control can effectively solve the problem of nonlinearity and rapid change and minimize the influence of disturbance and parameter change. It does not rely on the precise mathematical model of the controlled object; besides it can overcome the influence of nonlinear factors and has a strong robustness to the parameter changes of the controlled object. It does not need to establish a mathematical model. According to the input and output result data of the actual system and referring to the operating experience of field operators, the system can be controlled in real time [18]. Its fuzzy PID control flow chart is as shown in Figure 9 below, and its wheelchair rotation speed can be obtained by the encoder.

The adaptive fuzzy pid quantifies and fuzzifies the input quantity, which is the deviation E between the set output voltage and the feedback voltage of the motor and the deviation change rate E_c . Seven fuzzy control states are used to describe the speed deviation E in the motor speed regulation fuzzy controller system: Negative Big (NB), Negative Medium (NM), Negative Small (NS), Zero (ZO), Positive Small (PS), Medium (PM), and Positive Big (PB). The corresponding universe of fuzzy sets after discretization is as follows: $E^* = \{-6, -5, -4, -3, -2, -1, 0, 1, 2, 3, 4, 5, 6\}$. The fuzzy control rules of DC motors are summarized in Table 1, with a total of 49 control rules [19].

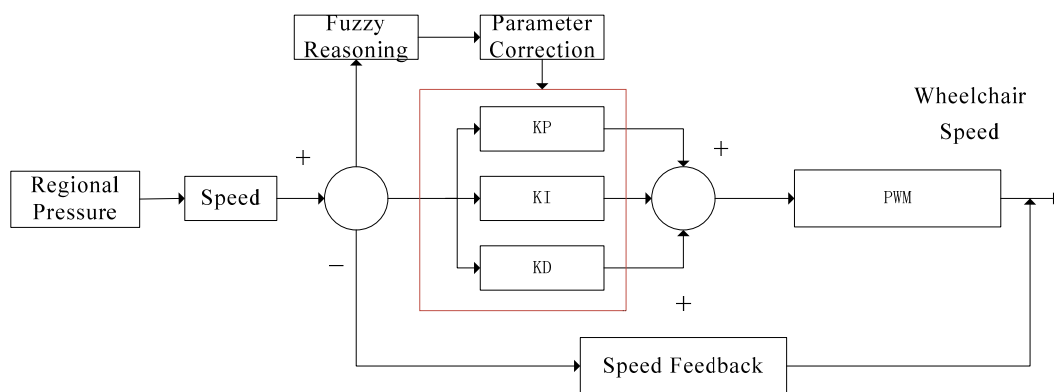


Figure 9. Fuzzy control flow chart.

Table 1. Fuzzy control rule table (U).

E_c	E						
	NB	NM	NS	ZO	PS	PM	PB
NB	NB	NB	NB	NB	NM	ZO	ZO
NM	NB	NB	NB	NB	NM	ZO	ZO
NS	NM	NM	NS	ZO	PS	PM	PM
ZO	NM	NS	ZO	PM	PM	PM	PM
PM	ZO	ZO	PM	PB	PB	PB	PB
PB	ZO	ZO	PM	PB	PB	PB	PB

The fuzzy relation of the output control system is:

$$R_i = A_i \times B_i \times C_i \tag{8}$$

$$R = \bigcup_{i=1}^n R_i = \bigcup_{i=1}^n (A_i \times B_i \times C_i) \tag{9}$$

The parameters of the PI controller are determined by the engineering design method, and the output u_i^* of the fuzzy PID controller obtained from the figure is:

$$u_i^* = u_i + u_f \tag{10}$$

$$u_i = K_i \sum_i e_i \tag{11}$$

$$u_f = f(e, e_c) \tag{12}$$

4.3. Anti-Misoperation Pressure Threshold Setting

First the average simulated mis-touch tongue muscle pressure were collected by four different experimenters using a carbon nanotube-PDMS pressure sensor (the simulated mis-touch tongue muscle pressure included the situation when the experimenters sit in a wheelchair and bump, or they swallow saliva normally). For each experimenter, we measure three times for bumping on the wheelchair as well as normal swallowing of saliva, respectively, and then collect the pressure under normal touch. Each experimenter normally touched the pressure sensor three times, and the experimental results are shown in Table 2. According to the data in the table below, we can conclude that when the pressure is greater than 0.12 N, the pressure signal is the action signal.

Table 2. Normal touch pressure and mis-touch tongue pressure collection form currently.

Number of Experiments	Pressure Data	Object			
		A	B	C	D
1	Normal pressure	0.124	0.138	0.131	0.127
	Swallowing saliva pressure	0.042	0.048	0.041	0.043
	Bump pressure	0.022	0.025	0.029	0.021
2	Normal pressure	0.122	0.132	0.135	0.129
	Swallowing saliva pressure	0.05	0.063	0.061	0.057
	Bump pressure	0.024	0.027	0.022	0.035
3	Normal pressure	0.128	0.139	0.134	0.132
	Swallowing saliva pressure	0.037	0.042	0.036	0.034
	Bump pressure	0.028	0.027	0.024	0.022

5. System Testing and Evaluation

In order to evaluate the performance of the device, an accelerated response time test and a central strike experiment are conducted. In order to test the performance of the system, six not-disabled subjects wear the system to perform two tasks for two different algorithm experiments: the speed response over time test, and a center click task [20]. Three healthy men and three healthy women perform the experiment, none of whom has ever used a tongue machine interface device before the experiment. In addition, a 20-s calibration is performed at first use, after which the subjects perform the following tasks according to the test content, respectively.

5.1. Speed Response Time Test

In this test, the response time of the speed control command is detected, and the speed response curve of wheelchair acceleration with time is obtained by matlab simulation.

When a DC motor with a set speed of 750 r/min reaches the steady state, the rise time of the traditional PID model is 0.14 s and the adjustment time is 0.64 s, while the rise time of the adaptive fuzzy PID is 0.108 s, and the adjustment time is 0.59 s. Compared with the traditional PID, the adaptive fuzzy PID control algorithm is more stable in the robustness of this system. Figure 10 shows the simulink model of PID and adaptive fuzzy PID, and Figure 11 shows the simulation results.

The results show that compared with the PID control algorithm, by adopting the fuzzy adaptive PID control algorithm, the system may reduce the overshoot and the time to reach the set speed of the wheelchair during the acceleration process.

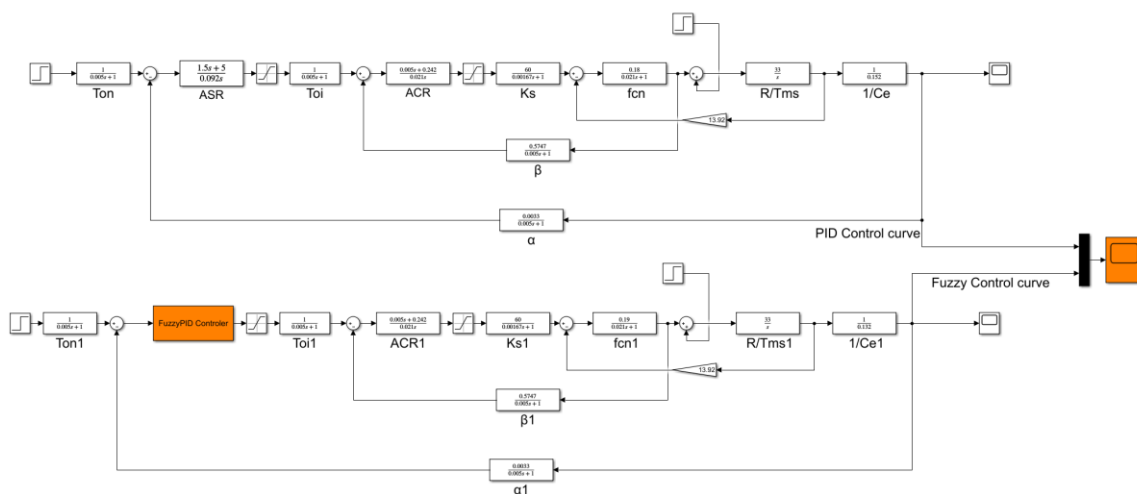


Figure 10. PID and adaptive fuzzy PID simulation.

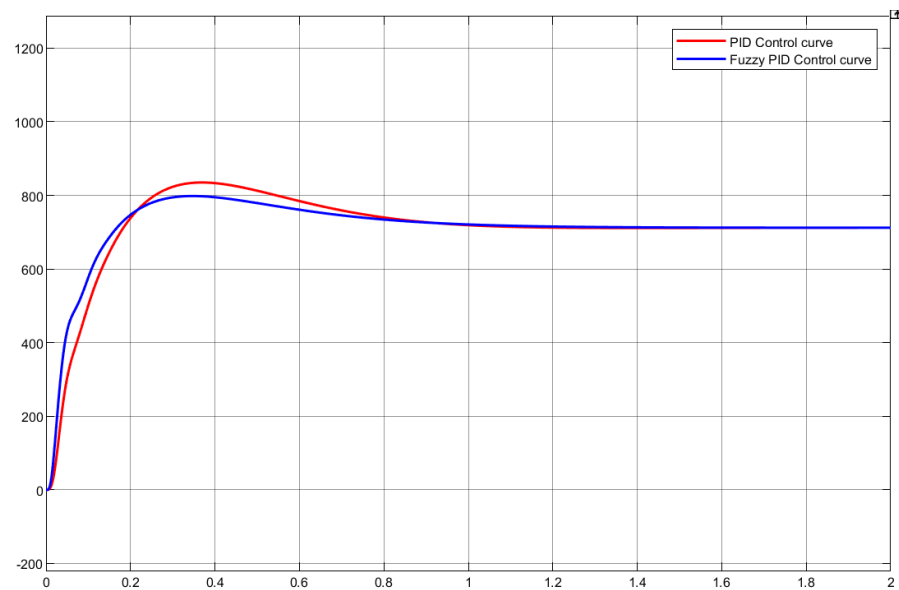


Figure 11. Simulation results.

5.2. Center Click Task Testing

The center click task evaluates tongue-controlled devices by speed and precision based on Fitts' law, which states the time to move a pointer to a target is related to the distance D between the current position of the pointer device and the target position and the size S of the target, as shown in Figure 12. The expression formula is:

$$t = a + b \log^2\left(\frac{D}{S} + 1\right) \quad (13)$$

where a , b represent empirical parameters which are based on the physical characteristics of the pointer device, the subject, and the environment [21].

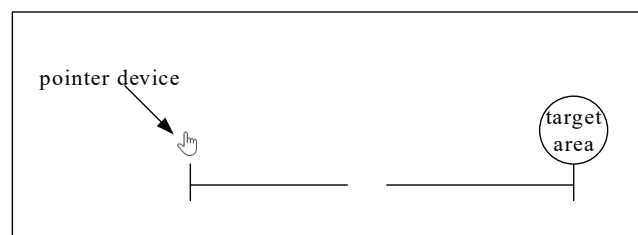


Figure 12. Schematic diagram of Fitts' law.

According to the method described by Fanpeng Kong et al. [22], two circular targets of different diameters are given randomly as 30 and 60 pixels, respectively. The target appears only one at a time at various distances from the center. Subjects manually manipulated the cursor to move from the center to the target and click on the center of the target as possible as they could. A total of 32 circular targets were randomly presented according to the subjects' clicks, as shown in Figure 13. In this paper, throughput and reaction time are used as reference indexes.

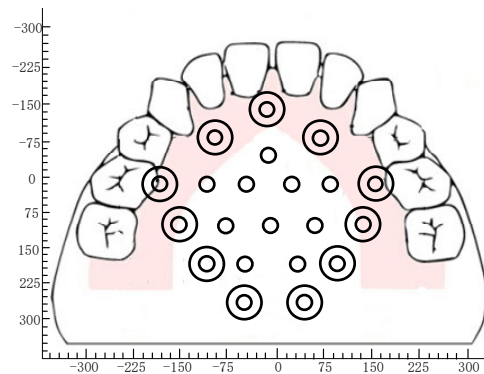


Figure 13. Center click task.

In this paper, throughput is used to represent the information transfer rate from the system to the laptop computer, which is in bits/s. The average throughput is given by the following equation:

$$t = a + b \log^2\left(\frac{D}{S} + 1\right) \quad (14)$$

$$TP = \frac{1}{n} \sum_{i=1}^n \left(\frac{1}{m} \sum_{j=1}^m \frac{ID_{ij}}{MT_{ij}} \right) \quad (15)$$

Among them, ID represents the difficulty index under the same conditions; MT represents the mean movement time; m represents the target number of subjects; n represents the total number of subjects, and the difficulty index under the same conditions is calculated according to Shannon's formula:

$$ID = \log^2\left(\frac{D}{W} + 1\right) \quad (16)$$

where D represents the distance from the pointer device, that is, the manual operation pointer, to the center of the circular target, and W represents the diameter of the circular target.

Response time refers to the time for the system to operate the cursor movement, represented by RT , and the unit is second.

The error rate refers to the proportion of subjects who fall outside the target range when they click on the target, expressed in ER .

From the above results, it can be observed that the throughput of tongue-controlled devices based on RSIC-V edge computing is less than that of iSTD devices and eTDS devices because the raw data of tongue-controlled devices based on RSIC-V edge computing has been processed on the sensor side and specific instructions have been generated, which greatly reduces the requirements for the data-transmission rate and thus reduces the loss of CPU occupancy and energy in data transmission; the reaction time of tongue-controlled devices based on RSIC edge computing in the central click task averages to be 0.16 s, which is faster than that of iSTD devices (0.457 s) and eTDS (0.227 s) devices.

Subjects performed 30 tongue touch tasks using iSTD, eSTD, and RSIC-V edge-based tongue control device, respectively, and the analysis results are shown in Figures 14 and 15 below.

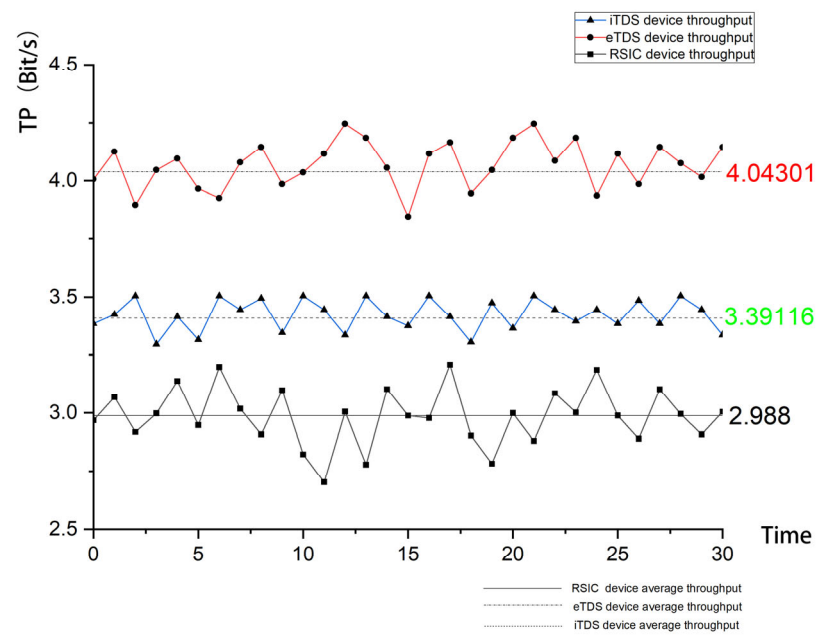


Figure 14. Hand and tongue system handling throughput of central click task.

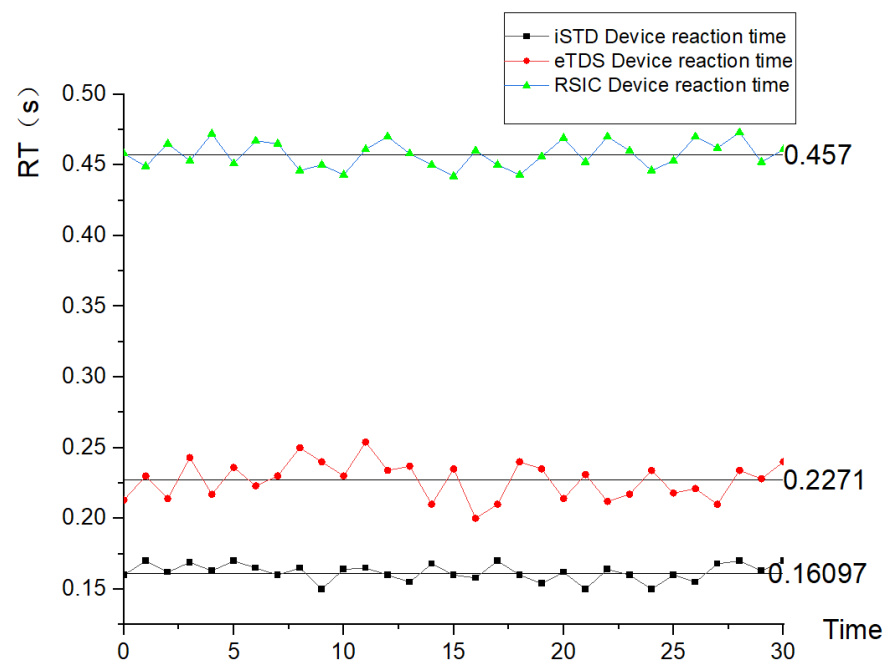


Figure 15. Operation reaction time of hand and tongue machine system in the center click task.

5.3. Power Consumption Test Comparison

The power consumption of the system is tested in the state of normal sending commands and standby as shown in Table 3 below:

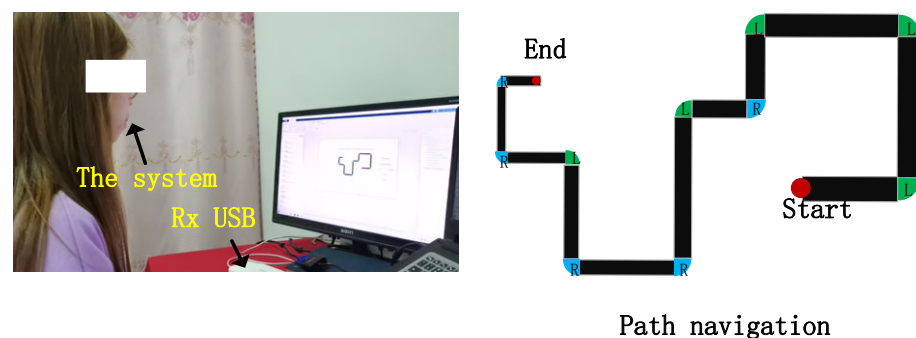
Table 3. Power consumption analysis of non-invasive intraoral independent tongue control system based on RSIC-V edge computing.

Type	Power Consumption (Mw)	
	Typical	Best
Network dynamic	3.300	3.100
Gate dynamic	0.270	0.264
I/O dynamic	0.075	0.060
Core static	0.138	0.015
Bank static	0.054	0.003
Memory	0.460	0.380
Total static	0.242	0.118
Total dynamic	3.745	3.424
Total	3.987	3.542

The low-power wearable independent tongue drive system (sTDS) developed by Ali Jafari et al. has a dynamic power consumption of 4.451 MW and a total power consumption of 4.471 MW. In this paper, the dynamic power consumption of the tongue control device is 3.745 MW, with a total power consumption of 3.987 MW. Compared to this, the dynamic power consumption in this article has been reduced by 18.8%, and the total power consumption has been reduced by 11.5%.

5.4. Labyrinth Navigation Task Experiment and Analysis

The maze navigation task is used to test the sensitivity of the system and is represented by controlling the total time the target passes through a fixed path. As shown in Figure 16, the subject sits in front of the computer, and the computer displays a GUI; the ultimate goal of this experiment is to move the ball from the starting point to the endpoint. The subjects conducted six maze experiments using iSTD devices, eTDS devices, and tongue control devices in this study, with a time of 2 min each time. If they exceeded the time limit, they did not complete the task. The experimental results are shown in Table 4. The bottom of the bar chart represents the average time taken by the subject to complete each of the six tasks.

**Figure 16.** Schematic diagram of maze navigation experiment.

From the results described in the above table, it can be observed that the average time taken to complete the experiment of the tongue control device in this article is 65.8 s, which is less than compared to iSTD devices and eTDS devices.

Table 4. Comparison table of labyrinth experiment time for multilingual control equipment.

Type of Tongue Control Device	Completion Time of the First Experiment (s)	Completion Time of the Second Experiment (s)	Completion Time of the Third Experiment (s)	Completion Time of the Fourth Experiment (s)	Completion Time of the Fifth Experiment (s)	Completion Time of the Sixth Experiment (s)	Average Experimental Completion Time (s)
iSTD	76	73	69	72	70	76	72.6
eTDS	83	97	86	83	79	82	85
This device	68	65	60	70	65	67	65.8

6. Conclusions

In this paper, a non-intrusive intraoral stand-alone tongue control system based on RSIC-V edge computing is proposed. Patients can detect the pressure signal of tongue muscle touching the palate through a flexible carbon nanotube-PDMS pressure sensor array placed in the mouth, avoid the occurrence of false movement signals through the setting of pressure threshold, and perform adaptive fuzzy PID control on the wheelchair through the normal tongue touching pressure. It can accurately control the movement of the wheelchair, thus increasing the reliability of the device and improving the user's experience. After many system tests, it is proved that the tongue-controlled system control scheme studied in this paper is reasonable. The problem of tongue control miscontact is solved, the data transmission is reduced, and the power consumption is reduced by 11.5% compared with the sTDS system. On the whole, the tongue-driven system placed in the mouth can achieve better use results after reasonable training and practice. Due to some limitations, improvements can be made in the following areas for future research: (1) The tongue control auxiliary device designed in this article simplifies the setting of tongue muscle pressure threshold. If time permits in the future, the sample tongue muscle pressure capacity should be increased and combined with algorithms that meet the conditions to set the threshold more scientifically. (2) The tongue control auxiliary device designed in this article requires an external power supply, which has brought some inconvenience to patients in practical application. Therefore, the packaging method of implantable power supply in the oral cavity needs to be studied.

Author Contributions: Investigation, J.Z. and L.W.; Resources, J.Z. and T.A.; Data curation, X.P.; Writing—original draft, X.P.; Writing—review & editing, L.S. and Z.K.; Supervision, L.S., J.Z. and Z.K.; Project administration, L.S.; Funding acquisition, J.Z. All authors have read and agreed to the published version of the manuscript.

Funding: This work was supported in part by the Jilin Provincial Department of Science and Technology (Grant/Award Number: No. YDZJ202303CGZH01, YDZJ202301ZYTS496), Jilin Provincial Department of Human Resources and Social Security (2022QN05), The Education Department of Jilin Province (No. JJKH20230673KJ) and Changchun Science and Technology Bureau (21ZGM29) in this article.

Institutional Review Board Statement: Not applicable.

Informed Consent Statement: Not applicable.

Data Availability Statement: Not applicable.

Conflicts of Interest: The authors declare no conflict of interest.

References

1. Sudeep, K.T.; Arun, S.B.; Jatadhara, G.S.; Majumder, A.; Dhar, A. Design and Fabrication of Rehabilitation-based Exoskeleton for Paralytic Arm. In Proceedings of the International Conference on Smart Electronics and Communication (ICOSEC), Trichy, India, 10–12 September 2020. [[CrossRef](#)]
2. Kong, F.; Sahadat, N.; Ghovanloo, M.; Durgin, G.D. A Stand-Alone Intraoral Tongue-Controlled Computer Interface for People with Tetraplegia. *IEEE Trans. Biomed. Circuits Syst.* **2019**, *13*, 848–857. [[CrossRef](#)] [[PubMed](#)]
3. Mohammadi, M.; Knoche, H.; Gaihede, M.; Bentsen, B.; Struijk, L.N.S.A. A high-resolution tongue-based joystick to enable robot control for individuals with severe disabilities. In Proceedings of the IEEE 16th International Conference on Rehabilitation Robotics (ICORR), Toronto, ON, Canada, 24–28 June 2019. [[CrossRef](#)]

4. Dang, B.; Purohit, B.; Sarang, D.; George, K. Tongue driven wireless electronic communication device. In Proceedings of the IEEE Sensors Applications Symposium (SAS), Glassboro, NJ, USA, 13–15 March 2017. [[CrossRef](#)]
5. Qui, N.M.; Lin, C.H.; Chen, P. Design and Implementation of a 256-Bit RISC-V-Based Dynamically Scheduled Very Long Instruction Word on FPGA. *IEEE Access* **2020**, *8*, 172996–173007. [[CrossRef](#)]
6. Shea, C.; Mohsenin, T. Heterogeneous Scheduling of Deep Neural Networks for Low-power Real-time Designs. *ACM J. Emerg. Technol. Comput. Syst. (JETC)* **2019**, *15*, 36. [[CrossRef](#)]
7. Akhter, F.; Siddiquei, H.R.; Alahi, M.E.E.; Mukhopadhyay, S.C. Design, Fabrication, and Implementation of a Novel MWC-NTs/PDMS Phosphate Sensor for Agricultural Applications. In Proceedings of the International Conference on Computational Intelligence and Computing, Jhansi, India, 19–20 February 2021; pp. 303–308. [[CrossRef](#)]
8. Zhang, K.; Shi, X.; Chen, J.; Xiong, T.; Jiang, B.; Huang, Y. Self-healing and stretchable PDMS-based bifunctional sensor enabled by synergistic dynamic interactions. *Chem. Eng. J.* **2021**, *412*, 128734. [[CrossRef](#)]
9. Trujilho, L.; Saotome, O.; Öberg, J. Dependable I2C Communication with FPGA. In Proceedings of the Brazilian Technology Symposium, Sao Paulo, Brazil, 8–10 November 2021; Springer: Cham, Switzerland, 2022.
10. Wu, H.; Pi, J.; Liu, Q.; Liang, Q.; Qiu, J.; Guo, J.; Long, Z.; Zhou, D.; Wang, Q. All-Inorganic Lead Free Double Perovskite Li-Battery Anode Material Hosting High Li⁺ Ion Concentrations. *J. Phys. Chem. Lett.* **2021**, *12*, 4125–4129. [[CrossRef](#)] [[PubMed](#)]
11. Sahadat, M.N.; Dighe, S.; Islam, F.; Ghovanloo, M. An Independent Tongue-Operated Assistive System for Both Access and Mobility. *IEEE Sens. J.* **2018**, *18*, 9401–9409. [[CrossRef](#)]
12. Barlow, S.; Custead, R.; Lee, J.; Hozan, M.; Greenwood, J. Wireless Sensing of Lower Lip and Thumb-Index Finger ‘Ramp-and-Hold’ Isometric Force Dynamics in a Small Cohort of Unilateral MCA Stroke: Discussion of Preliminary Findings. *Sensors* **2020**, *20*, 1221. [[CrossRef](#)] [[PubMed](#)]
13. Yadav, R.; Zhang, W.; Elgendy, I.A.; Dong, G.; Shafiq, M.; Laghari, A.A.; Prakash, S. Smart Healthcare: RL-Based Task Offloading Scheme for Edge-Enable Sensor Networks. *IEEE Sens. J.* **2021**, *21*, 24910–24918. [[CrossRef](#)]
14. Ferdian, R.; Aisuwarya, R.; Erlina, T. Edge Computing for Internet of Things Based on FPGA. In Proceedings of the International Conference on Information Technology Systems and Innovation (ICITSI), Bandung, Indonesia, 19–23 October 2020. [[CrossRef](#)]
15. Izci, D. Design and application of an optimally tuned PID controller for DC motor speed regulation via a novel hybrid Lévy flight distribution and Nelder–Mead algorithm. *Trans. Inst. Meas. Control.* **2021**, *43*, 3195–3211. [[CrossRef](#)]
16. Ekinci, S.; Izci, D.; Eker, E.; Abualigah, L. An effective control design approach based on novel enhanced aquila optimizer for automatic voltage regulator. *Artif. Intell. Rev.* **2023**, *56*, 1731–1762. [[CrossRef](#)]
17. Zand, J.P.; Sabouri, J.; Katebi, J.; Nouri, M. A new time-domain robust anti-windup PID control scheme for vibration suppression of building structure. *Eng. Struct.* **2021**, *244*, 112819. [[CrossRef](#)]
18. Tunjung, D.; Prajitno, P.; Handoko, D. Temperature and water level control system in water thermal mixing process using adaptive fuzzy PID controller. *J. Phys. Conf. Ser.* **2021**, *1816*, 012032. [[CrossRef](#)]
19. Aftab, A.; Luan, X. A fuzzy-PID series feedback self-tuned adaptive control of reactor power using nonlinear multipoint kinetic model under reference tracking and disturbance rejection. *Ann. Nucl. Energy* **2022**, *166*, 108696. [[CrossRef](#)]
20. Engwall, O. Combining MRI, EMA and EPG measurements in a three-dimensional tongue model. *Speech Commun.* **2003**, *41*, 303–329. [[CrossRef](#)]
21. Kim, J.; Park, H.; Bruce, J.; Rowles, D.; Holbrook, J.; Nardone, B.; West, D.P.; Laumann, A.E.; Roth, E.; Veledar, E.; et al. Qualitative assessment of Tongue Drive System by people with high-level spinal cord injury. *J. Rehabil. Res. Dev.* **2014**, *51*, 451–465. [[CrossRef](#)] [[PubMed](#)]
22. Kong, F.; Jia, Y.; Ghovanloo, M. Preliminary Assessment of a Novel Intraoral-Tongue Operated Assistive Technology with Computer Interface. In Proceedings of the IEEE 63rd International Midwest Symposium on Circuits and Systems (MWSCAS), Springfield, MA, USA, 9–12 August 2020. [[CrossRef](#)]

Disclaimer/Publisher’s Note: The statements, opinions and data contained in all publications are solely those of the individual author(s) and contributor(s) and not of MDPI and/or the editor(s). MDPI and/or the editor(s) disclaim responsibility for any injury to people or property resulting from any ideas, methods, instructions or products referred to in the content.